Atmospheric Research 135–136 (2014) 314–321

Contents lists available at ScienceDirect

Atmospheric Research

journal homepage: www.elsevier.com/locate/atmos

Microwave radio emissions of negative cloud-to-ground lightning flashes

D. Petersen *, W. Beasley

University of Oklahoma School of Meteorology, 120 David L. Boren Blvd. Suite 5900, Norman, OK, USA

ARTICLE INFO

Article history:
Received 6 August 2012
Received in revised form 31 January 2013
Accepted 6 February 2013

Keywords:
Lightning discharge
Lightning radiation
Dart leader
Negative stepped leader
Return stroke

ABSTRACT

We report preliminary results of a new observational study of microwave-frequency electromagnetic radiation that is emitted by lightning discharge processes. Radiation was observed with a ceramic patch antenna and a digital radio receiver tuned to a center frequency of 1.63 GHz and a bandwidth of 2 MHz. The recorded radiation waveforms are compared with data collected by the Oklahoma Lightning Mapping Array (OKLMA) lightning mapping system and the co-located Earth Networks Total Lightning Network (ENTLN) broadband electric field antenna. Microwave radiation was observed to occur during preliminary breakdown, negative stepped leader breakdown, negative dart leader breakdown, and return strokes. Characteristic radiation signatures were observed, including trains of individually resolvable impulses during breakdown and brief but intense trains of noise-like bursts during return strokes.

1. Introduction

Lightning is an important manifestation of severe weather, causing a significant portion of severe weather damage. The state of the understanding of lightning is broad and in some instances detailed, but numerous questions remain. Current research involving lightning physics is focused on understanding of processes such as initiation, positive and negative leader breakdown, dart leader breakdown, and runaway breakdown. One of the most important means of studying lightning processes has been observations of the resultant electromagnetic emissions, especially at radio frequencies (RF). There are numerous studies, too numerous to list here, that detail observations made from near DC through VHF and lower UHF frequencies. The reader may refer to the text by Rakov and Uman (2003) for a thorough review of these studies. At frequencies above about 1 GHz, however, there are relatively few studies.

The part of the RF spectrum ranging from 1 GHz up to about 10 GHz is still relatively transparent in heavy precipitation environments (Janssen, 1993), so there exists a potential for observing lightning processes at these frequencies. Based on a theoretical analysis, Cooray and Cooray (2011) have reported that the electron avalanche, a fundamental process of electrical discharges, is capable of generating significant radiation in the microwave band. The earliest observational studies at microwave frequencies include those by Ligda (1956) who reported observations of RF impulses at 10 GHz, and by Atlas (1959) who reported observations of RF impulses at 1.2 and 2.8 GHz. Brook and Kitagawa (1964) reported observations at 0.85 GHz with a bandwidth of 200 kHz, reporting radiation coincident with negative stepped leader, return stroke, dart leaders, K changes, and IC discharges. Stepped leaders were shown to generate strong impulsive radiation with easily discernible pulses, while dart leaders were also seen to radiate strongly but with the pulses often overlapping. Return strokes were also seen to radiate strongly, but not all of the time. IC discharge activity was also observed to emit radiation, and was often seen to radiate more strongly than during CG discharges. Oetzel and Pierce (1968) reported observations of RF impulses at 11 GHz, 90 MHz, and VLF, showing that nearly all microwave emissions occur as a few brief impulses during some, but not all, return strokes. The radiation pulses were shown to be only a few microseconds in duration. Radiation was also observed in

* Corresponding author. Tel.: +1 405 325 7411.
E-mail address: danp@ou.edu (D. Petersen).

0169-8095/$ – see front matter © 2013 Elsevier B.V. All rights reserved.
http://dx.doi.org/10.1016/j.atmosres.2013.02.006

association with leader breakdown, with an intensity that was an order of magnitude weaker than that of the accompanying return strokes. Kosarev et al. (1970) reported observations at 0.7 GHz, 0.9 GHz and 1.3 GHz with a 1 MHz bandwidth using omnidirectional dipole antennas, showing bursts of radiation at 0.7 and 0.9 GHz with durations in the order of 10 ms. Radiation was detected at 1.3 GHz, but was considered insufficient for analysis. Rust et al. (1979) reported observations at 2.2 GHz and a bandwidth of 500 kHz using a high-gain parabolic antenna, showing impulsive activity during leader breakdown, return strokes and dart leaders. Le Boulch et al. (1987) reported observations at 900 MHz and 4.6 GHz and a bandwidth of 128 kHz, showing radiation during some (but not all) return strokes. Due to the relatively narrow bandwidth of the receiver, impulse width could not be resolved. Most recently, Yoshida (2008) reported observations at VHF and at 2.9 GHz with a bandwidth of 500 kHz using a standard gain horn antenna. Analysis of a single flash that was initiated on a tall radio tower showed radiation associated with an upward-propagating positive leader, subsequent dart leader/return stroke sequences, and late intracloud breakdown activity. The initial upward positive leader was observed to generate impulsive radiation at both VHF and microwave frequencies, as were the dart leaders. The return strokes were observed to be quiet in the VHF band while generating a strong burst of radiation at 2.9 GHz with the burst showing a much higher impulse frequency than during the leader breakdown. A period of impulsive activity was also observed during a continuing current phase that was associated with intracloud activity. At the higher end of the microwave spectrum, Fedorov et al. (2001) observed radiation at 37.5 GHz with a 1 MHz bandwidth using a high-gain dish antenna. Impulse trains were detected in conjunction with the passage of a lightning channel through the beam, but it was unclear whether the radiation was generated by leader breakdown or by the return stroke.

Upon review of these studies, it is clear that various lightning discharge processes radiate well at microwave frequencies. Given the impulsive nature of this radiation, it is important to note that all of these studies involved receiver bandwidths less than 1 MHz. Such bandwidths limit the time resolution of impulse width to about 1 μs, limiting the ability to observe impulses whose pulse width is much less. Observations of dE/dt waveforms by Murray et al. (2005), and of UHF radiation by Labaune et al. (1987) and Bondiou et al. (1987) show that a significant fraction of impulses have pulse widths in the order of tens of nanoseconds. The existence of such narrow impulses suggests that the ability to detect impulsive radiation from lightning may be greatly enhanced by a suitable increase in receiver bandwidth. It was suggested by Oetzel and Pierce (1968) that lightning-generated radiation at frequencies above 200 MHz could not be observed using omnidirectional antennas and available receivers. They also suggested that receiver bandwidths greater than a few hundred kilohertz would be unnecessary for resolving individual impulses. Possibly because of these expectations, most studies at microwave frequencies have been conducted using highly directional antennas and relatively narrow bandwidths. However, given improvements in modern receiver noise figures and the low cost for digitizing signals with wide bandwidths, it is reasonable to explore the possibility of using omnidirectional antennas in order to observe lightning discharge processes at microwave frequencies. We expect that with a sufficiently low receiver noise figure and wide receiver bandwidth, it will be possible to map the impulsive radiation generated by lightning at microwave frequencies using both time-of-arrival and interferometry techniques. The observations reported in this paper represent the first iteration of our effort, and support these expectations.

2. Observational apparatus

A diagram of the apparatus is shown in Fig. 1.

The apparatus consisted of a roof-mounted antenna, LNA and filter connected via shielded coaxial cable to a nearby digital radio receiver system. A commercially available GPS ceramic patch antenna, shown in the left-hand side of Fig. 2, was utilized for its cardioid antenna pattern and circular polarization. A cardioid radiation pattern exhibits maximum gain in the forward direction, with the gain falling off by approximately 10 dB at 90° from the forward direction. Circular polarization allows for non-preferential reception of all orientations of linearly polarized radiation, with overall attenuation of 3 dB. For the observations reported in this study, the antenna was vertically oriented and located at the top of the south-facing wall of the National Weather Center in Norman, OK, as shown in the right-hand side of Fig. 1.

The antenna was connected via a short hardline coaxial cable to a low noise amplifier with 23.5 dB gain and a noise figure just over 2 dB. The signal was filtered and then transported via coaxial cable to a nearby laboratory where it was again filtered, amplified and then fed into a digital radio receiver. The receiver was an Ettus Research USRP1 with a DBSRX2 direct-conversion front end, an analog-to-digital (A/D) converter, and a field-programmable gate array (FPGA) DSP processor. The daughter board amplified and mixed the received signal, generating both in-phase (I) and quadrature (Q) baseband components that were fed to the A/D converter where they were linearly sampled at a bit depth of 12 bits and a sampling rate of 64 MHz. The digitized I and Q signals were then passed to the FPGA processor where they were decimation low-pass filtered to a bandwidth of 2 MHz and then resampled at 2 MS/s and 16 bits. The resulting baseband I and Q signals were then passed by a USB 2.0 trans port to a host computer where they were stored on a hard drive for later analysis. In order to maintain accurate timing of the incoming signals, a GPS-disciplined IRIG-B signal was fed into a parallel channel of the USRP and was synchronously recorded as a time reference. The microwave signals were later demodulated to a magnitude waveform. The system was not calibrated, therefore it is not possible to attach an accurate value to the received signal amplitude. Further complicating this problem, the ceramic patch antenna was oriented upward but the flashes discussed in this paper were located at a range of lower elevation angles. Based on the given manufacturer specifications, the system had an estimated signal gain (not including antenna gain) of 72 dB and an estimated noise figure of 3–4 dB.

In order to interpret the microwave data, comparisons were made with a co-located Earth Networks Total Lightning Network (ENTLN) electric field waveform antenna and the Oklahoma Lightning Mapping Array (OKLMA) lightning mapping system. The ENTLN waveform antenna has a pass band of 1 Hz to 12 MHz, enabling the capture of both slow and fast electric field waveform records. It also has GPS timing, allowing precise

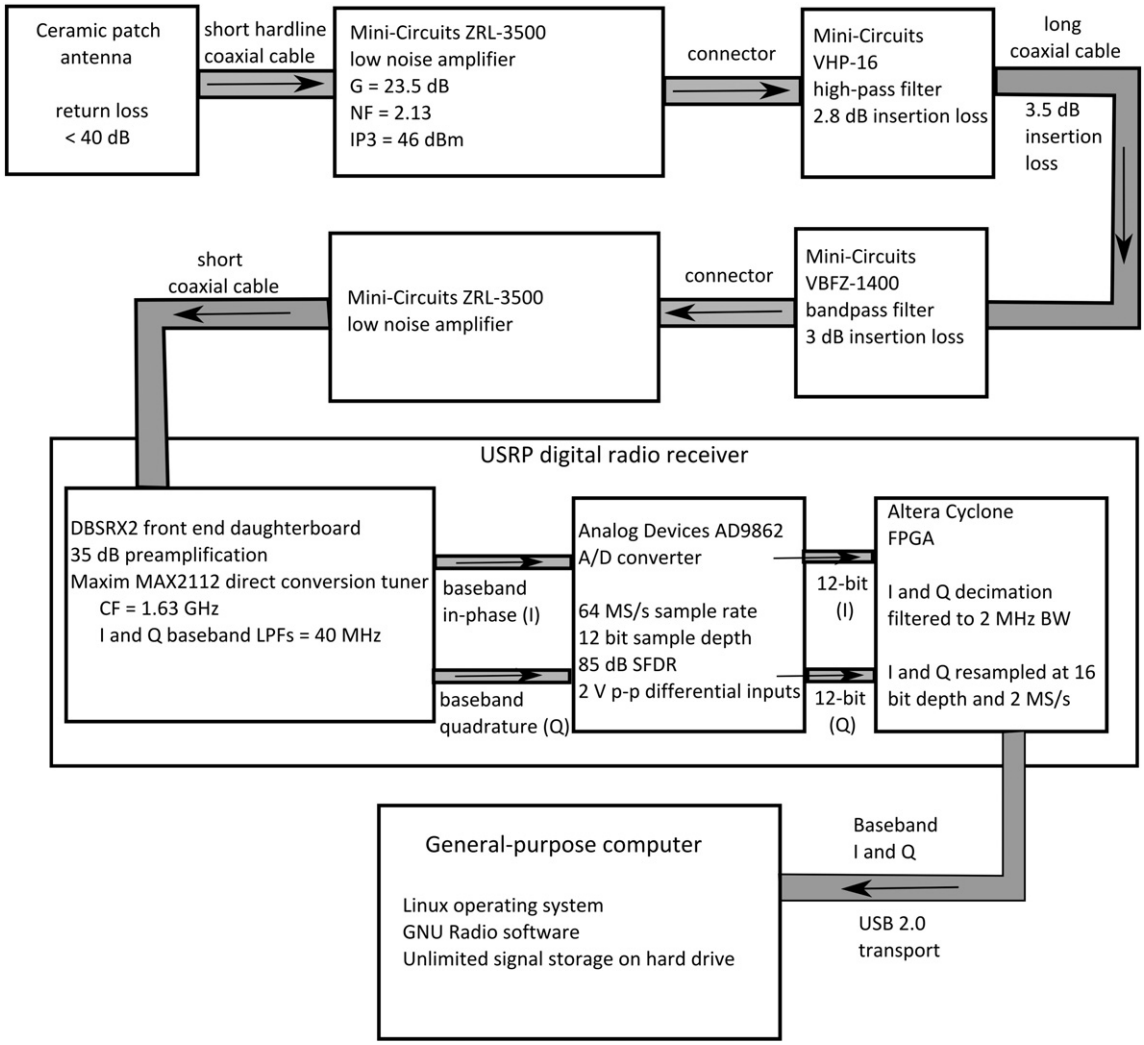

Fig. 1. Diagram of the observational apparatus. The system was not calibrated, but based on manufacturer specifications it had an estimated total front-end amplification of 72 dB and an estimated noise figure of 3–4 dB.

comparison of waveforms to other similarly timed data such as that reported in this paper. Calibration information was not available for the ENTLN waveforms. The OKLMA utilizes multiple receiving stations and precise GPS-based timing of impulsive VHF radiation at each station to create a single 3-D + time map of the source locations of the VHF signals. A detailed description of the general lightning mapping array (LMA) system can be found in Rison et al. (1999).

Fig. 2. The left photograph is a top-down view of the system front end. A GPS patch antenna is mounted on a 100 mm^2 ground plane and is connected via a short coaxial hardline to a low-noise amplifier and filter. The right photograph shows the antenna as it was positioned during observations. The antenna was oriented vertically, giving a maximum antenna gain in the vertical direction and a gain reduction in the horizontal direction of approximately 10 dB.

3. Observations and discussion

Fig. 3 is an LMA plot of part of a lightning flash that occurred just south of the National Weather Center on 05-20-2011 at 5:29:23 UTC. The plot shows two descending negative stepped leaders of a single negative cloud-to-ground flash. Two separate connections to the ground can be seen: the first connection was approximately 6 to 8 km south of the microwave antenna while the second connection was approximately 2 km south of the microwave antenna.

Fig. 4 is a comparison of the LMA time vs. altitude plot from Fig. 3 with the microwave signal. The microwave radiation generated during the descent of the negative stepped leaders consisted of trains of individual impulses (only partially resolvable in Fig. 4), while the return strokes consist of more intense bursts of impulsive noise.

Fig. 5 is a magnified view of the period immediately prior to and during the second return stroke displayed in Fig. 4. Microwave radiation during the descent of the negative stepped leader was generated as a series of individually resolvable impulses superposed on a more continuous elevated background noise, while the radiation during the return strokes was generated as a more continuous and more intense burst. Upon completion of the return stroke, the microwave radiation quickly subsided to low pre-flash background noise levels. Due to the system bandwidth of 2 MHz, the resolvability of individual impulses is limited to 500 ns. Due to this limitation, it cannot be determined if the elevated background noise during the leader phase, or the radiation burst during the return stroke phase, are truly continuous or are simply an unresolvable series of individual impulses.

Fig. 6 is an LMA plot of part of a lightning flash that occurred just south of the National Weather Center on 05-20-2011 at 5:29:53 UTC. The plot shows a sequence of negative leaders and return strokes during a single negative cloud-to-ground flash. The return strokes were located 5 to 6 km south of the microwave antenna. The LMA data shows at least three long-duration descending negative leader impulse trains that were followed by return strokes, with another two apparent return strokes preceded by little preliminary impulsive activity.

Fig. 7 is a comparison of the LMA time vs. altitude plot from Fig. 3 with the microwave signal. Two phenomena are

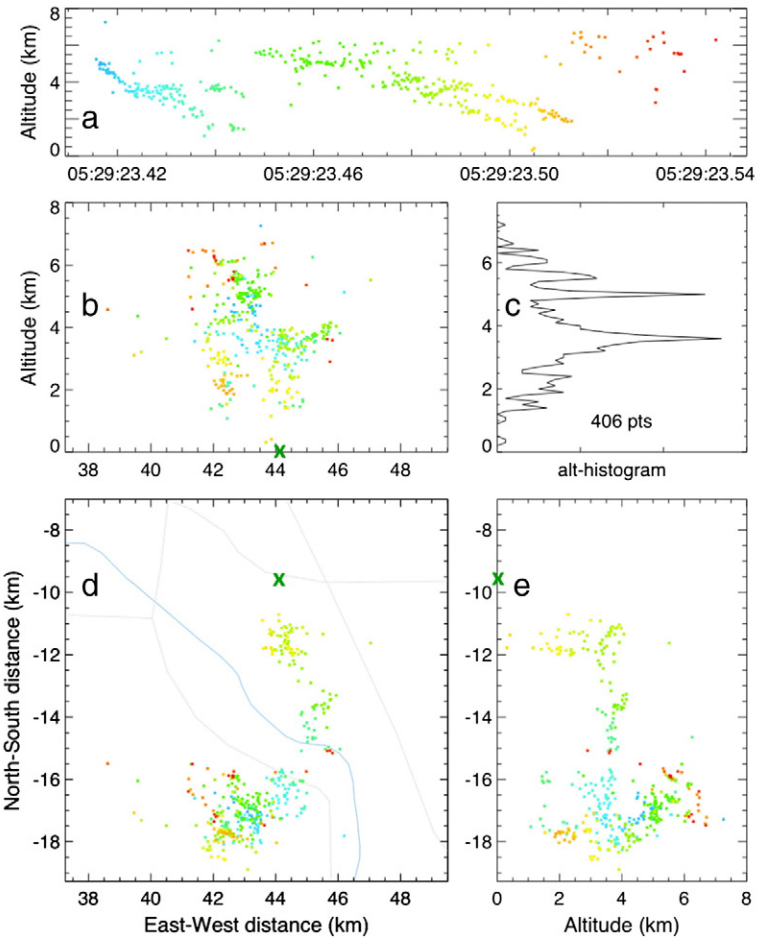

Fig. 3. LMA plot of a lightning flash that occurred on 5-20-2011 at 5:29:23 UTC south of the National Weather Center. The green X indicates the position of the microwave receiver. Plot a is a time vs. altitude plot showing two descending negative stepped leaders. Plot d is a top-down projection of the flash, while plots b and e are side-projections.

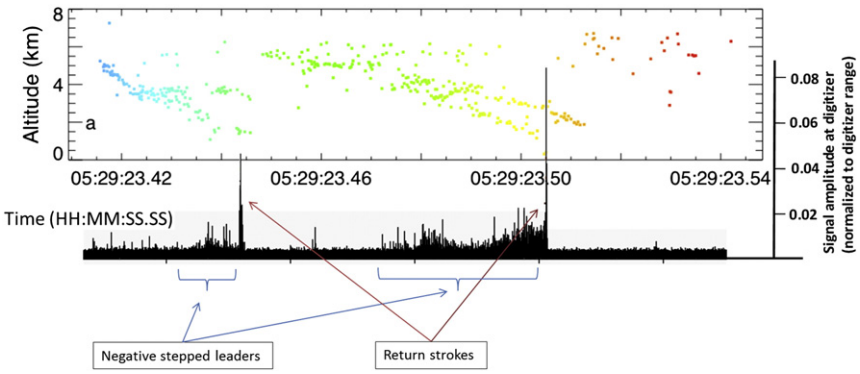

Fig. 4. Time-series comparison of LMA VHF source heights (upper point plot) and corresponding microwave intensity (lower line plot). Descending negative stepped leaders can be seen on the LMA plot as a sequential lowering to ground level of VHF source locations. Impulsive radiation at microwave frequencies was observed during the development of the descending negative stepped leader. Strong but brief increases in microwave intensity were observed to occur upon cessation of the descending OKLMA source points, indicating strong microwave radiation during return strokes.

of particular interest in this case. First is the series of precursor impulses that occurred before onset of the initial negative stepped leader. These impulses were relatively weak and narrow, and were clearly distinguishable from the stepped leader impulses based on their relative isolation in time and their individual narrowness.

Also of interest is the strong microwave radiation event near the end of the record. The event was dominated by a

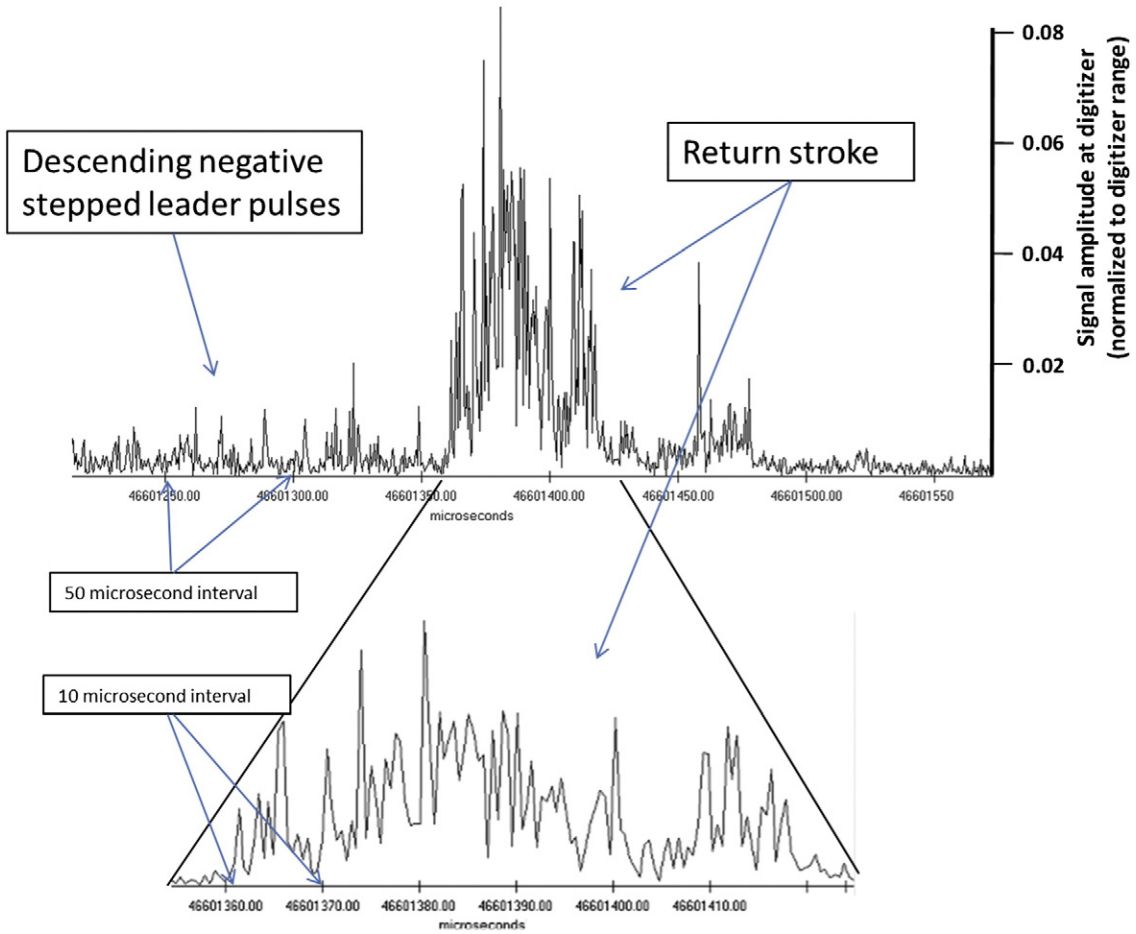

Fig. 5. Magnified view of the second return stroke shown in Fig. 4. The upper plot shows the impulsive activity prior to the return stroke corresponding to the descending negative stepped leader. The more intense burst of radiation during the return stroke is expanded in the lower plot, showing significant impulsive activity superposed on an apparent elevation of continuous emissions.

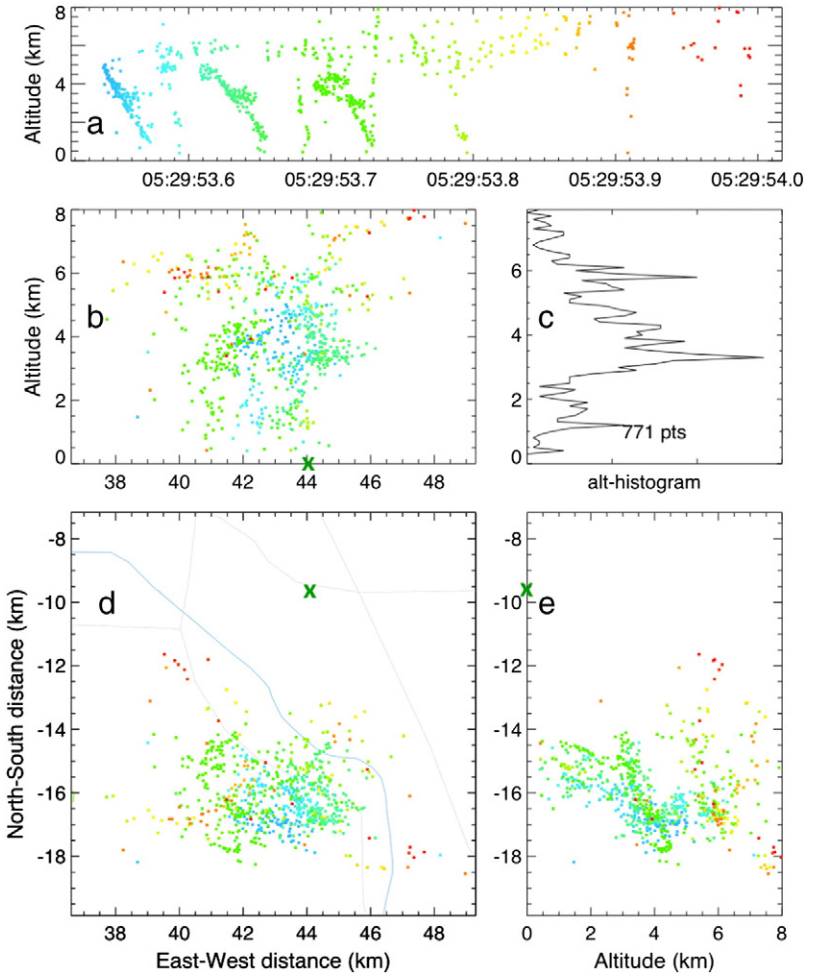

Fig. 6. LMA plot of a lightning flash that occurred on 5-20-2011 at 5:29:53 UTC south of the National Weather Center. The green X indicates the position of the microwave receiver. Plot a is a time vs. altitude plot showing two descending negative stepped leaders. Plot d is a top-down projection of the flash, while plots b and e are side-projections.

microwave signal with features that are characteristic of return strokes. However, unlike the earlier negative stepped leaders, the event was marked by the lack of corresponding OKLMA points. Fig. 8 is a magnified view of the microwave signal during this event, and includes the ENTLN fast electric field waveform for comparison.

A train of highly impulsive microwave radiation lasting 1 ms can be seen on both the microwave and electric field

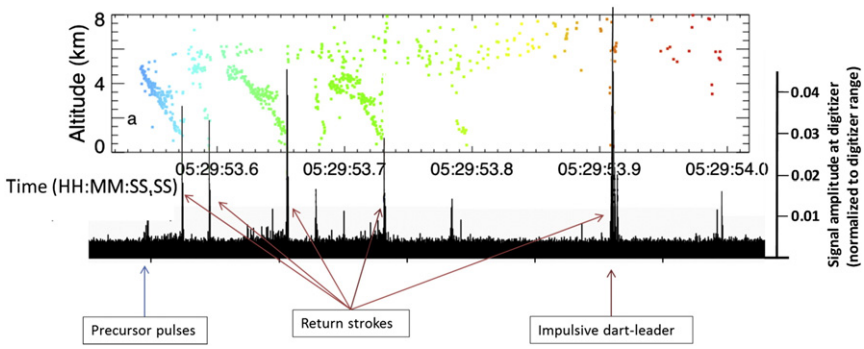

Fig. 7. Time-series comparison of LMA VHF source vertical locations (upper plot) and corresponding microwave intensity (lower plot). The two plots are overlapping in order to enable comparison. A series of descending negative stepped leaders can be seen in both the microwave and LMA records, and are followed by return strokes that are evident only in the microwave record. A few precursor pulses can be seen at the beginning of the microwave record, corresponding to the early stages of preliminary breakdown. The tall signal at 05:29:53.9 was clipped in this image, reaching a true height of 0.08 V.

records, and is immediately followed by an intense noise burst at microwave frequencies and a strong electric field change corresponding to a return stroke. The time scale of the impulsive train is an order of magnitude shorter than that of a typical descending negative stepped leader, but is typical of a dart leader suggesting the event to be an impulsive dart leader. The impulses of this event were stronger than those of the earlier descending negative stepped leaders, and occasionally disappeared for short periods of time during the final stages before the return stroke. The ENTLN fast electric field waveform contains impulsive bursts during the impulsive phase and return stroke, followed by a more slowly varying component suggestive of a continuing current mode. Microwave radiation was quickly reduced to background levels with a few intermittent bursts after the return stroke, even though the electric field waveform shows continued activity. This suggests that the drainage of current during the continuing current phase following a return stroke only intermittently includes processes that radiate significantly at microwave frequencies.

4. Conclusions

This study reports the preliminary results of an investigation of lightning-generated microwave radiation at 1.63 GHz. The results show that significant microwave radiation is radiated by lightning during preliminary breakdown, negative stepped leader breakdown, impulsive dart leader breakdown, and return strokes. Preliminary breakdown, negative stepped leaders and impulsive dart leaders were observed to generate trains of individually resolvable impulses, while return strokes were observed to generate stronger but more continuous noise-like bursts. A distinct signature was observed during preliminary breakdown, where a few isolated and relatively strong impulses appeared several milliseconds before onset of the more closely spaced train of negative stepped leader impulses. This suggests that the initial breakdown processes of a lightning flash may be different from those that occur during development of the negative stepped leader. Intermittent impulsive radiation was observed during an apparent dart leader, suggesting a physical similarity to the negative stepped leader. However, the larger impulse intensity and impulse frequency suggests that significant difference remain. Also of interest during the dart leader event was a period of no impulsive radiation just prior to the return stroke. The time structure of all of the microwave observations was limited by the 2 MHz bandwidth of the baseband signal. This limitation may obscure more rapid impulsive radiation, either hiding it or causing it to appear as continuous noise-like radiation. This possibility is supported by similar observations of fast electric field waveforms by Labaune et al. (1987) and Bondiou et al. (1987), where the timescale of some impulses was observed in the order of tens of nanoseconds.

The observations presented in this paper confirm and expand on earlier studies of lightning-generated RF radiation at microwave frequencies. Comparison of microwave radiation with the OKLMA VHF point source location maps and the ENTLN electric field waveforms allows for identification of characteristic microwave radiation signatures for various lightning discharge processes. The microwave receiver system bandwidth of 2 MHz has offered a much improved time resolution of the microwave signals compared to previous studies, but uncertainties remain. Future efforts will include increasing the bandwidth of the system by an order of magnitude or more in order better resolve the time scale of individual impulses and overlapping impulse trains. Future attention will also be directed toward identifying

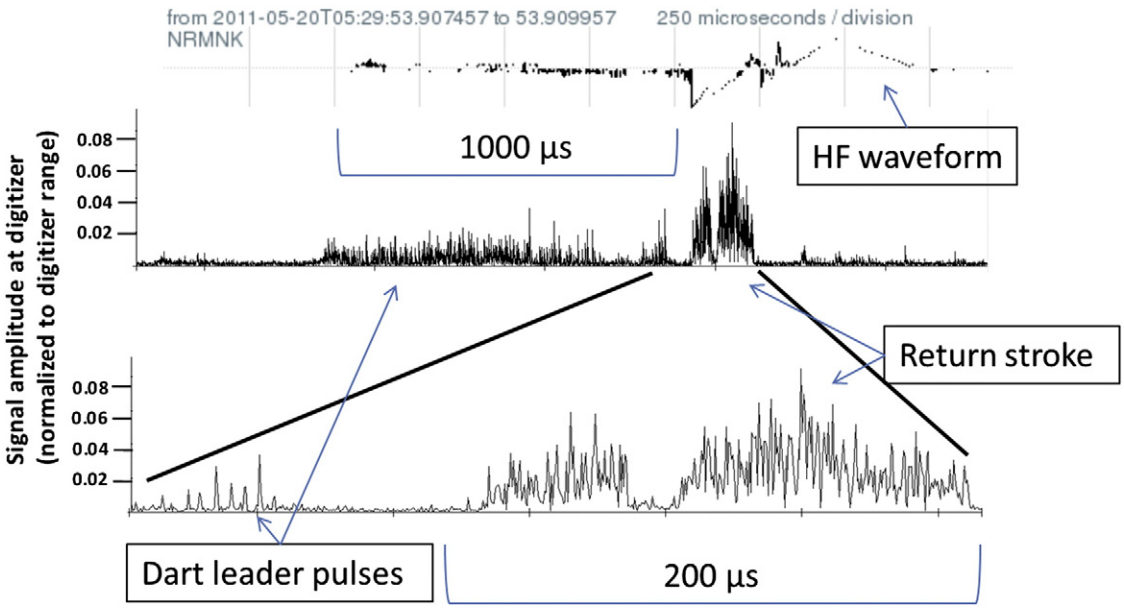

Fig. 8. Magnified view of the period just prior to and during the return stroke at 05:29:53.9 in Fig. 7. The middle plot shows a train of impulsive microwave radiation followed by a shorter burst of more intense noise-like radiation that is likely due to a return stroke. The lower plot shows a further magnified view of the strong radiation burst and the period immediately preceding it. The upper plot is the ENTLN fast electric field waveform, showing small impulses followed by a large negative excursion indicative of a negative return stroke.

the microwave signatures of specific processes such as lightning initiation, positive leader breakdown, first and subsequent return strokes and intracloud discharges.

Acknowledgments

Support for this research was provided by the DARPA Nimbus Program, the National Science Foundation, Division of Atmospheric Sciences, under grant number 0721119, the University of Oklahoma Vice President for Research, the OU School of Meteorology, and the Oklahoma State Regents for Higher Education.

References

Atlas, D., 1959. Radar lightning echoes and atmospherics in vertical cross-section. Recent Advances in Atmospheric Electricity. Pergamon Press, London, pp. 441–459.

Bondiou, A., Labaune, G., Marque, J.P., 1987. Electromagnetic radiation associated with the formation of an electric breakdown in air at atmospheric pressure. J. Appl. Phys. 61 (2), 503–509.

Brook, M., Kitagawa, N., 1964. Radiation from lightning discharges in the frequency range 400 to 1000 Mc/s. J. Geophys. Res. 69 (12), 2431–2434.

Cooray, V., Cooray, G., 2011. Electromagnetic radiation field of an electron avalanche. Atmos. Res. http://dx.doi.org/10.1016/j.atmosres.2011.06.004.

Fedorov, V.F., Frolov, Y.A., Shishkov, P.O., 2001. Millimetric electromagnetic radiation of a lightning return stroke. J. Appl. Mech. And Tech. Phys. 42 (3), 392–396.

Janssen, M.A., 1993. Atmospheric Remote Sensing by Microwave Radiometry. John Wiley and Sons, Inc., New York, N. Y.

Kosarev, E.L., Zatsepin, V.G., Mitrofanov, A.V., 1970. Ultrahigh frequency radiations from lightning. J. Geophys. Res. 75 (36), 7524–7530.

Labaune, G., Richard, P., Bondiou, A., 1987. Electromagnetic properties of lightning channels formation and propagation. Electromagnetics 7, 361–393.

Le Boulch, M., Hamelin, J., Weidman, C., 1987. UHF-VHF radiation from lightning. Electromagnetics 7, 287–331.

Ligda, M.G.H., 1956. The radar observation of lightning. J. Atmos. Terr. Phys. 9, 329–340.

Murray, N., Krider, P., Willett, J., 2005. Multiple pulses in dE/dt and the fine-structure of E during the onset of first return strokes in cloud-to-ocean lightning. Atmos. Res. 76, 455–480.

Oetzel, G.N., Pierce, E.T., 1968. The radio emissions from close lightning. Planet. Electrodyn. 1, 543–571.

Rakov, V.A., Uman, M.A., 2003. Lightning: Physics and Effects. Cambridge University Press0521583276.

Rison, W., Thomas, R.J., Krehbiel, P.R., Hamlin, T., Harlin, J., 1999. A GPS-based three-dimensional lightning mapping system: initial observations in central New Mexico. Geophys. Res. Lett. 26 (23), 3573–3576.

Rust, W.D., Krekbiel, P.R., Shlanta, A., 1979. Measurements of radiation from lightning at 2200 MHz. Geophys. Res. Lett. 6 (2), 85–88.

Yoshida, S., 2008. Radiations in Association with Lightning Discharges, Ph. D. Thesis, Osaka University, Japan.